Journal of Biomechanics 85 (2019) 92–100

Contents lists available at ScienceDirect

Journal of Biomechanics

journal homepage: www.elsevier.com/locate/jbiomech
www.JBiomech.com

Myocardial bridging and endothelial dysfunction – Computational fluid dynamics study

Ashkan Javadzadegan [a,b,*], Abouzar Moshfegh [a,b,1], Yi Qian [a], Leonard Kritharides [b,c], Andy S.C. Yong [a,b,c]

[a] Faculty of Medicine and Health Sciences, Macquarie University, Sydney, NSW 2109, Australia
[b] ANZAC Research Institute, The University of Sydney, Sydney, NSW 2139, Australia
[c] Department of Cardiology, Concord Hospital, The University of Sydney, Sydney, NSW 2139, Australia

ARTICLE INFO

Article history:
Accepted 8 January 2019

Keywords:
Myocardial bridging
Endothelial dysfunction
Computational fluid dynamics
Wall shear stress

ABSTRACT

Myocardial bridging (MB) is associated with endothelial dysfunction in patients with angina and non-obstructive coronary artery disease. This study aims to determine if there is a link between abnormal blood flow patterns and endothelial dysfunction in patients with MB. Ten patients with MB in their left anterior descending (LAD) artery were selected, 5 of whom had endothelial dysfunction and 5 had no endothelial dysfunction based on their response to acetylcholine. Similarly, 10 patients without MB in their LAD, 5 of whom had endothelial dysfunction and 5 of whom had no endothelial dysfunction, were studied as a control group. Transient computational fluid dynamics simulations were performed to derive wall shear stress (WSS) over the entire vessel including proximal, middle and distal segments. Patients with MB and endothelial dysfunction had lower WSS in the proximal LAD and greater WSS in the mid-LAD than patients with MB but without endothelial dysfunction. When comparing patients with endothelial dysfunction, those with MB had significantly lower shear stress in the proximal LAD (0.32 ± 0.14 Pa (with MB) vs 0.71 ± 0.38 Pa (without MB), p = 0.01) and greater shear stress in the mid-LAD (2.81 ± 1.20 Pa (with MB) vs 1.66 ± 0.31 Pa (without MB), p = 0.014) than patients without MB. Our findings demonstrated that the presence of MB significantly contributes to low WSS and endothelial dysfunction relationship.

1. Introduction

Myocardial bridging (MB) is a congenital anomaly that refers to the condition whereby an epicardial coronary artery dives into the cardiac musculature for a section of its course. MB is associated with coronary endothelial dysfunction in patients with chest pain and non-obstructive coronary artery disease (CAD) (Masuda et al., 2001; Wang et al., 2004; Zoghi et al., 2006; Kim et al., 2008; Chatzizisis and Giannoglou, 2009; Corban et al., 2014).

Almost two-thirds of patients with non-obstructive CAD have evidence of endothelial dysfunction (Radico et al., 2014; Sara et al., 2015). It has been theorised that low wall shear stress (WSS) causes endothelial dysfunction in these patients (Malek et al., 1999; Puri et al., 2015; Weber and Noels, 2011). However, there are only few studies that explored the WSS and endothelial dysfunction relationship in vivo (Kumar et al., 2018; Siasos et al., 2018). Kumar et al. (2018) demonstrated for the first time that probability of severe endothelial dysfunction increases with decrease in WSS.

When it comes to patients with MB, there are only a handful of studies (Doriot et al., 2007; Nikolić et al., 2014; Ding et al., 2017) that used over-simplified in-silico and in-vitro models to derive shear stress in MB arteries. We addressed this issue in our previous study (Javadzadegan et al., 2018) in which we developed and validated an in silico model that accurately mimicked the three-dimensional and dynamic nature of MB. In the current study, we aim to implement the previously developed in silico model of MB to systematically explore the shear and endothelial dysfunction relationship in patients with non-obstructive CAD and to investigate if the presence of MB contributes to this relationship.

2. Materials and methods

2.1. Patient selection

Patients with angina who were referred to the cardiac catheterisation laboratory for coronary angiography were screened for the

* Corresponding author at: Faculty of Medicine and Health Sciences, Level 1, 75 Talavera road, Macquarie University, NSW 2109, Australia.
E-mail address: ashkan.javadzadegan@mq.edu.au (A. Javadzadegan).
[1] Joint first author.

https://doi.org/10.1016/j.jbiomech.2019.01.021
0021-9290/

presence of MB. All patients were screened for the presence of MB in the LAD artery. Ten patients with MB in their LAD were selected, 5 of whom had endothelial dysfunction and 5 had no endothelial dysfunction based on their response to acetylcholine (ACh). Ten patients without MB in their LAD, 5 of whom had endothelial dysfunction and 5 of whom had no endothelial dysfunction, were also studied as a control group. Intravascular ultrasound (IVUS) was performed in all selected patients. Written informed consent was obtained from all patients, and the study was approved by the Human Research Ethics Committee at our institution.

2.2. Quantitative coronary angiography and coronary physiology measurements

Coronary angiogram was performed with cine images acquired at 15 frames per second (fps) as per convention at our institution. Quantitative coronary angiography (QCA) analysis was performed using Cardiovascular Angiography Analysis System (CAAS v5.11, Pie Medical Imaging, Maastricht, the Netherlands). QCA was used to reconstruct the LAD from its ostium to the most distal segment of the artery possible. In all patients (with and without MB) the full length of LAD was equally divided into 3 segments: proximal, middle and distal.

A Combowire (Volcano, San Diego, USA) was introduced into the LAD artery to obtain intracoronary pressure and velocity waveforms at rest and during peak stress, as previously described (Javadzadegan et al., 2018).

2.3. Coronary endothelial function testing

To assess for the presence of endothelial dysfunction and vasospasm, cine images were obtained in 2 orthogonal views at baseline and after slow intracoronary administration of 50 mcg of ACh, 100mcg of ACh and 200 mcg of glyceryl trinitrate sequentially. The ACh was infused over 2–3 min to induce maximal coronary hyperaemia. We did not proceed to higher dose of ACh if the lower dose resulted in vasoconstriction. Offline, QCA was performed and changes in coronary diameter (minimum lumen diameter, and mean lumen diameter) throughout the LAD were computed. Changes in the coronary diameter in response to ACh and glyceryl trinitrate coronary administration were expressed as the percentage change from the baseline of the angiogram. Endothelial dysfunction was diagnosed if the epicardial coronary artery diameter decreased by >0% at any location of the LAD compared to baseline (Suwaidi et al., 2000; Lee et al., 2015). The greatest paradoxical ACh response was considered for the diagnosis of endothelial dysfunction.

2.4. Intravascular ultrasound and MB characteristics

An IVUS recording from the distal LAD to the guide catheter was performed in a standard fashion using automated motorized pullback (0.5 mm/s) by a 40-MHz Atlantis Pro IVUS catheter (Boston Scientific, Marlborough, USA). The IVUS data were obtained for the first 50 mm of the LAD ostium and IVUS images were analysed using in-house developed software (Javadzadegan et al., 2018). Supplementary video 1 shows an example of analysis of IVUS images of a patient without MB using the in-house developed software. In this video, the pink color as well as (+) markers illustrate structure of static and dynamic masking systems. The red traces are for image segmentation and skeletonizing process resulted in binary skeletons of luminal border(s) in form of connected and/or disconnected edge traces (tracks), shown by green traces, which are separately identifiable.

For patients with MB, the presence of MB was defined either by the identification of an echolucent half-moon sign or evidence of systolic compression (Ge et al., 1999). Fig. 1 shows morphology of MB for a representative patient with bridging in the mid-LAD. Fig. 1A and B represent the angiographic images at end diastole and end systole where the total analysed length of LAD, the entrance and length of MB are marked. Fig. 1C and D show IVUS-captured cross-sectional images of the vessel in the bridge segment at end diastole and end systole where the bridge characteristics including halo thickness and arterial compression are depicted. Table 1 summarises the bridge characteristics of all patients included in this study.

2.5. Three-dimensional reconstructions of coronary arteries and CFD modelling

As described in our previous work (Javadzadegan et al., 2018), in-house software was used to reconstruct three-dimensional (3D) geometry of the vessel by fusion of angiography and IVUS. The workflow of fusion is shown in supplementary video 2. The reconstructed models were transferred to ANSYS CFX 15.0 (ANSYS Inc., Canonsburg, USA) for CFD analysis. The surface of the models were meshed using tetrahedral elements with a patch conforming method, and with a boundary layer mesh consisting of 4 layers with a height ratio of 1.2 (Prakash and Ethier (2001). A mesh dependency study was carried out with different element sizes as summarised in supplementary Table 1. The WSS averaged over proximal, bridge and distal segments were chosen as the control parameters for mesh dependency test (supplementary Fig. 1). As seen, refining the element size from 0.5 mm (Grid (I)) to 0.15 mm (Grid (V)) improved the results significantly (up to 50%); however, further refinement to 0.01 mm (Grid (VIII)), did not overly affect the results (0.61% to 3.03%). Therefore, to minimise the computational costs and to provide a high level of accuracy, Grid (V) was chosen for mesh generation.

Blood flow for the simulation was assumed to be Newtonian with dynamic viscosity of 0.0035 Pa s and density of 1050 kg/m^3, three-dimensional, unsteady and turbulent. Although in healthy coronary arteries, blood flow is laminar in nature, in the presence of a stenosis it may become turbulent (Ferrari et al., 2006). The MB can be considered as a dynamic stenosis as the bridge segment that goes intramurally through the myocardium is compressed during systole and creates a narrowing (Ishii et al., 1986). Notwithstanding that coronary arteries in this study have non-obstructive lesions and might often have laminar blood flow, they may experience turbulent flow due to the presence of MB. Therefore, shear stress transport (SST) turbulence model was used to capture the transition from laminar to turbulent, if any (Menter, 1994; Menter et al., 2006). SST model predicts the flow field in stenotic arteries more accurately than its traditional two-equation counterparts (k-omega and k-epsilon) (Varghese et al., 2008).

For haemodynamic simulation of patients with and without MB, the previously developed CFD model was used (Javadzadegan et al., 2018). In brief, a parametric moving-boundary algorithm was developed to simulate muscle compression caused by bridging and a rigid body algorithm was developed to model the non-bridge segments.

Fig. 2 illustrates the steps involved in constructing the CFD model of MB for the representative artery of Fig. 1.

(i) The parametric moving-boundary algorithm read bridge characteristics including bridge location, length and compression ratio (Fig. 2A), bridge and non-bridge segments (Fig. 2B), and electrocardiogram (ECG) and intracoronary velocity, proximal and distal pressure waveforms (Fig. 2C).
(ii) The moving-boundary algorithm determined, based on ECG, duration of systole (I-II, Fig. 2D) and diastole (II-IV, Fig. 2D) and applied a time-dependant force (F(t), Fig. 2B), synchro-

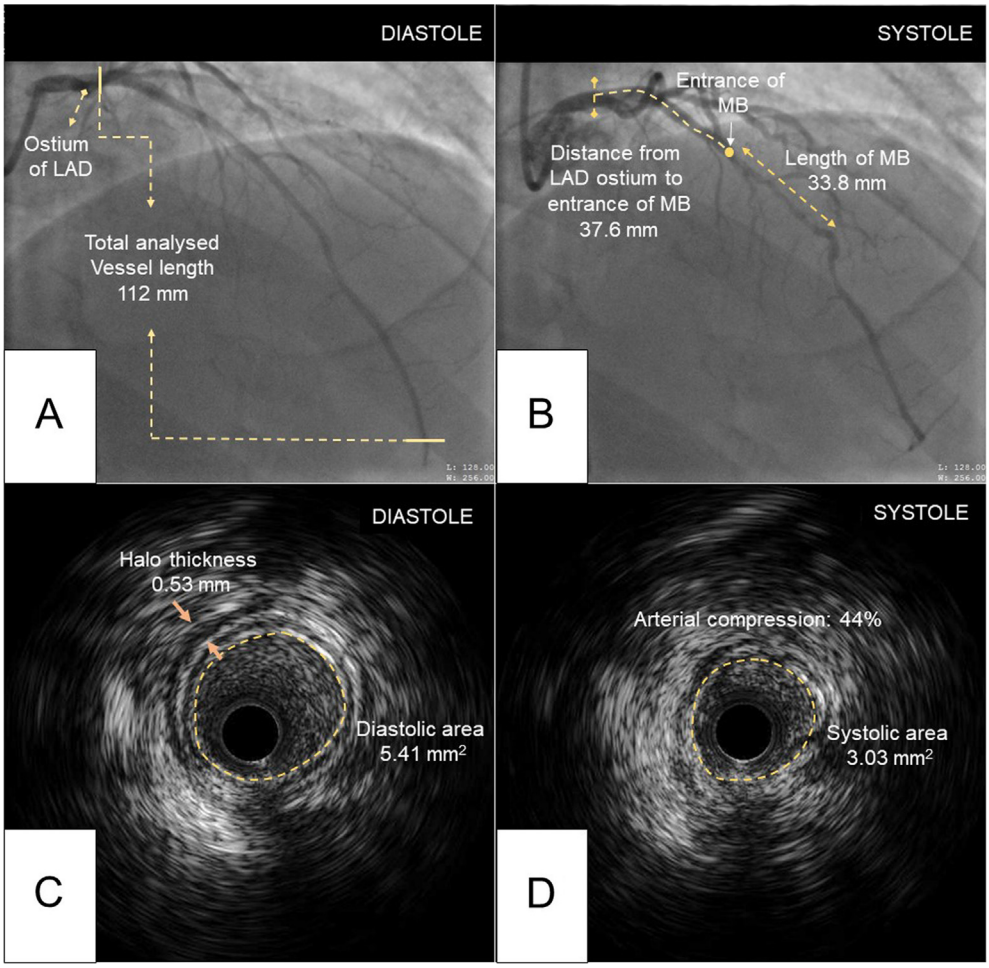

Fig. 1. A representative patient with MB in the mid LAD. (A) Angiography at end diastole, (B) angiography at end systole, (C) IVUS at end diastole, (D) IVUS at end systole.

Table 1
IVUS parameters of MB.

All MB cases (n = 10)	
Length of MB (mm)	32.9 ± 17.3
[1]Halo thickness (mm)	0.50 ± 0.25
[2]Systolic area (mm^2)	3.6 ± 0.99
[3]Diastolic area (mm^2)	5.7 ± 1.75
[4]Arterial compression (%)	36.6 ± 10.73
Distance from LAD ostium to entrance of MB	36.4 ± 13.1

[1] Maximal thickness of the echolucent band partially surrounding the artery, measured at end systole.
[2] The area of the artery at bridge segment at end systole.
[3] The area of the artery at bridge segment at end diastole.
[4] The decrease in external elastic membrane cross sectional area (CSA) at end systole standardized by external elastic membrane CSA at end diastole, expressed as a percentage.

nised with ECG, on the bridge segment. As previously known (Bourassa et al., 2003), extrinsic vessel compression due to MB is not only a systolic event, but also persists during a significant portion of the diastole. This is obvious from Fig. 2D where the vessel compression started from beginning of systole and continued till end of systole (I-II) and extended further into diastole (II-III).

(iii) The developed moving-boundary algorithm, applied on the bridge section, was coupled with rigid body algorithm, applied on the non-bridge parts. Both algorithms were then coupled to fluid flow governing equations.

(iv) Patient-specific proximal and distal pressure waveforms were used as inlet and outlet boundary conditions, respectively (Fig. 2C). The transient simulations were then run with a constant time step of 0.01 (s) over three cardiac cycles to satisfy the condition of periodic solution and results at the last cycle were used for haemodynamic analysis.

Supplementary video 3 illustrates the computer model of the representative artery of Fig. 1 with 2 bridges (MB (I) and MB (II)) in the middle segment that is synchronised with ECG as well as the corresponding angiography video. The characteristics of MB (I) and MB (II) are summarised in supplementary Table 2.

2.6. Statistical analysis

Graphpad Prism v. 7.01 (Graphpad, La Jolla, California) and SPSS v. 22 (IBM Corporation, New York, USA) software were used to perform statistical analyses. Normality of the data was determined using the D'Agostino Pearson test. Continuous variables were expressed as mean ± SD. Unpaired T-tests and one-way analysis of variance (ANOVA) were used to compare the means of continuous variables. A two-sided p value of <0.05 was considered significant.

3. Results

Baseline demographic, angiographic and physiological characteristics of all patients included in this study are summarised in

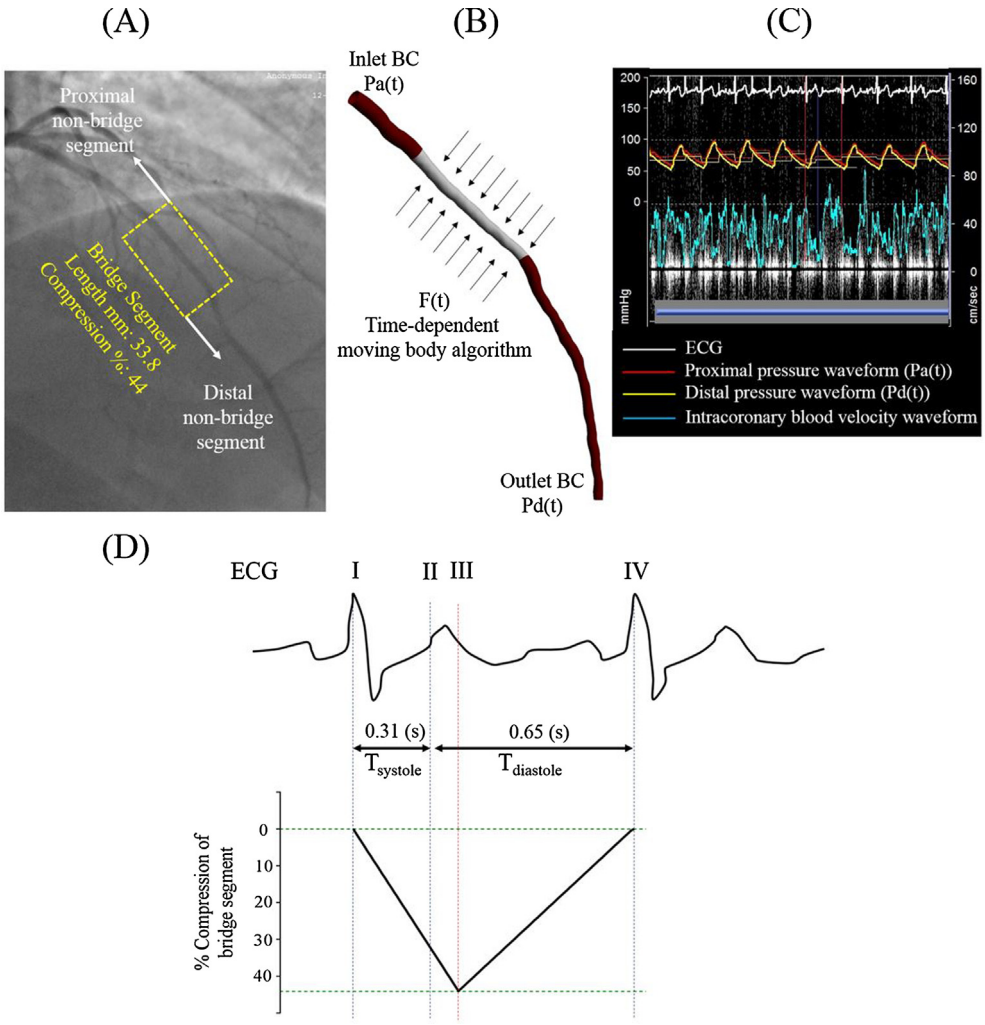

Fig. 2. The representative patient of Fig. 1. (A) Angiography at end diastole, (B) Computer model of MB. F(t) represents a time-dependant force applied on the bridge segment to compress it. (C) Intracoronary pressure and velocity measurements. Coronary blood velocity (blue tracing), proximal pressure (red tracing) and distal pressure (yellow tracing), and ECG (white tracing). (D) Compression of bridge segment synchronised with ECG. (For interpretation of the references to color in this figure legend, the reader is referred to the web version of this article.)

Table 2. There was no significant difference between the total analysed length from the ostium of the LAD for patients with MB (n = 10) and without MB (n = 10) (119 ± 13.1 mm vs 104 ± 13.6 mm, p = 0.22). Baseline percentage diameter stenosis of patients with MB was slightly higher than that of patients without MB, but the different was not statistically insignificant (p = 0.10). There was no significant difference in demographic, angiographic and physiological characteristics of patients with MB (n = 10) and without MB (n = 10) (Table 2).

Percent change in MLD and mean lumen diameter after ACh administration in the proximal and middle LAD segments were significantly greater in patients with MB (n = 10) compared to those without (n = 10); however, there was no significant difference in the distal segment (Fig. 3A and B).

Fig. 4 shows two representative patients with a MB in the mid LAD, one with endothelial dysfunction in the mid LAD (Fig. 4A–F) and the other without (Fig. 4G–L). As seen, the WSS at end diastole and end systole in the mid LAD of the patient with endothelial dysfunction was almost 3 and 2 times respectively greater than those for the patient without endothelial dysfunction.

In patients with MB (n = 10), those with endothelial dysfunction had significantly lower WSS in the proximal segment and higher WSS in the middle segment (Fig. 5A and B). However, there was no significant difference in the distal WSS (Fig. 5C). As with patients with MB, the WSS in the mid-LAD of patients without MB (n = 10) was remarkably higher in those with endothelial dysfunction (Fig. 6B); however, there was no significant difference in the proximal and distal WSS (Fig. 6A and C).

When comparing patients with endothelial dysfunction, those with MB (n = 5) had significantly lower WSS over the proximal segment in comparison with those without MB (n = 5). In patients without endothelial dysfunction, however, there was no significant difference in proximal WSS of those with MB (n = 5) and without MB (n = 5) (Fig. 7).

4. Discussion

4.1. Endothelial dysfunction and low WSS

As outlined in a number of studies (Asakura and Karino, 1990; Gibson et al., 1993; Glagov et al., 1988; Sawchuk et al., 1994), the endothelial cells exposed to low/oscillatory shear stress are flat and polygonal and are therefore structurally dysfunctional. According to our results, when evaluating patients with endothelial dysfunction, those with MB had significantly lower shear stress in the proximal LAD compared to those without MB (Figs. 5A and 6A). However, in patients with healthy endothelium, no significant

Table 2
Baseline clinical, physiological and angiography characteristics.

Variable	All cases (n = 20)	With MB (n = 10)	Without MB (n = 10)	p
Age (yr)	51.8 ± 8.5	52.5 ± 7.7	50.9 ± 9.4	0.27
Sex (male), no (%)	6 (33)	3 (33)	3 (33)	0.88
Weight (kg)	81.4 ± 19.9	80.6 ± 20.1	81.9 ± 19.7	0.54
Resting proximal pressure (mmHg)	87.3 ± 14.8	83.1 ± 14.5	91.5 ± 14.7	0.41
Resting distal pressure (mmHg)	80.8 ± 12.9	76.9 ± 12.7	84.7 ± 12.8	0.21
Hyperaemic proximal pressure (mmHg)	74.7 ± 12	71.9 ± 11.9	77.4 ± 12.2	0.36
Hyperaemic distal pressure (mmHg)	64.5 ± 11.7	61.5 ± 11.1	67.4 ± 12.3	0.29
Fractional flow reserve (FFR)	0.86 ± 0.06	0.85 ± 0.06	0.87 ± 0.05	0.63
Coronary flow reserve (CFR)	4.28 ± 1.43	4.33 ± 1.28	4.25 ± 1.56	0.19
Index of microvascular resistance (IMR)	16.2 ± 4.94	16.48 ± 5.44	15.91 ± 4.42	0.11
Total analysed vessel length (mm)	111.0 ± 13.9	119 ± 13.1	104 ± 13.6	0.22
Diameter stenosis (%)	24.7 ± 6.58	27.57 ± 7.67	21.9 ± 3.58	0.10
Minimum lumen diameter (MLD) (mm)	1.24 ± 0.36	1.19 ± 0.32	1.28 ± 0.40	0.26

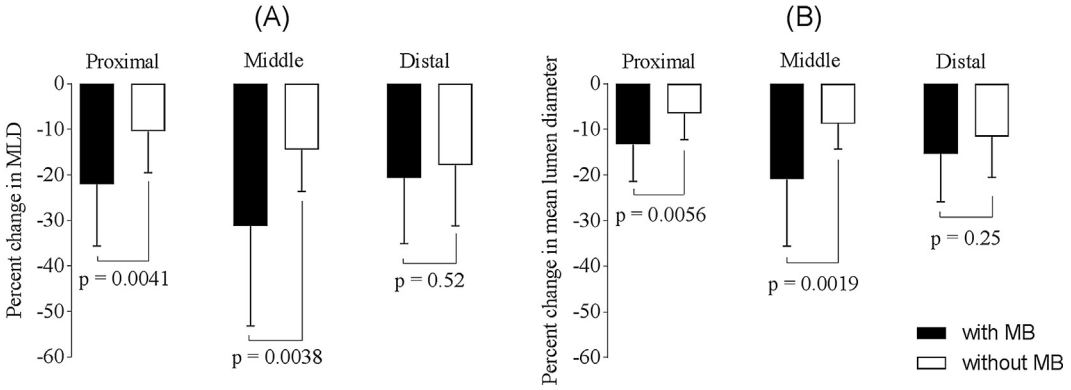

Fig. 3. Change in LAD MLD after ACh. (A) Percent change in MLD, (B) percent change in mean lumen diameter. Mean ± SD change after ACh in each group, "p" compares MB with no MB groups.

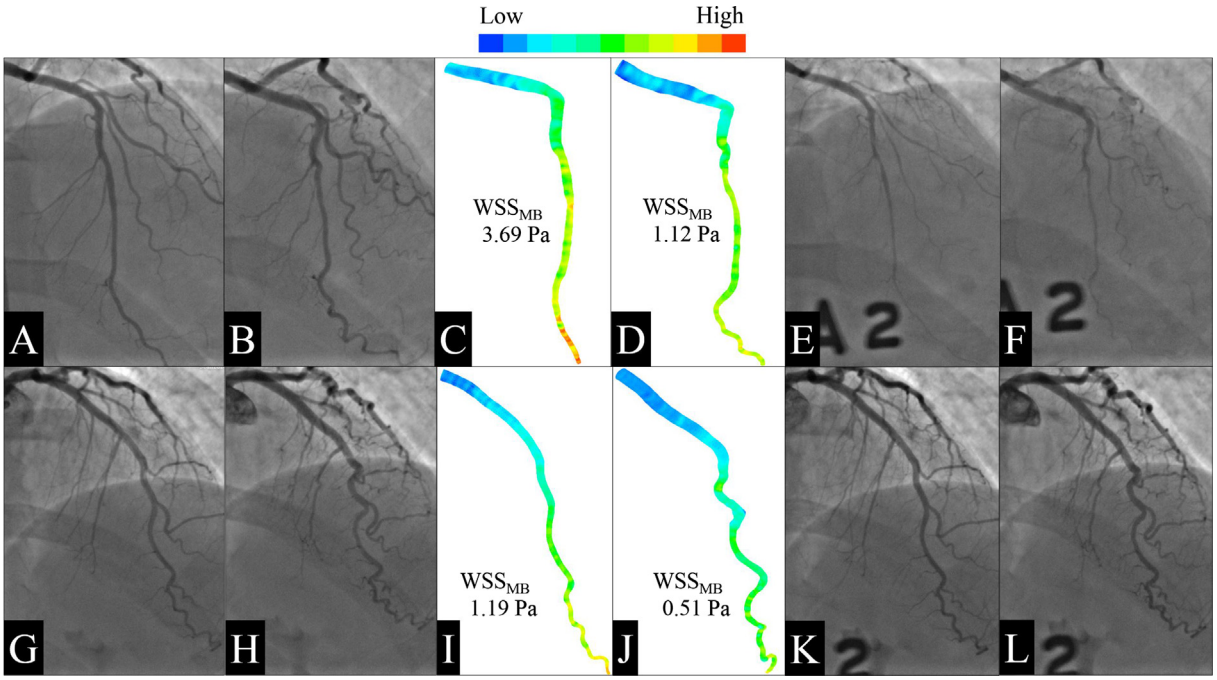

Fig. 4. Representative example of LAD with MB and with endothelial dysfunction. (A) End diastole, (B) End systole, (C) WSS contours at end diastole, (D) WSS contours at end systole, (E) Response to ACh at end diastole, (F) Response to ACh at end systole. Representative example of LAD with MB and without endothelial dysfunction. (G) End diastole, (H) End systole, (I) WSS contours at end diastole, (J) WSS contours at end systole, (K) Response to ACh at end diastole, (L) Response to ACh at end systole.

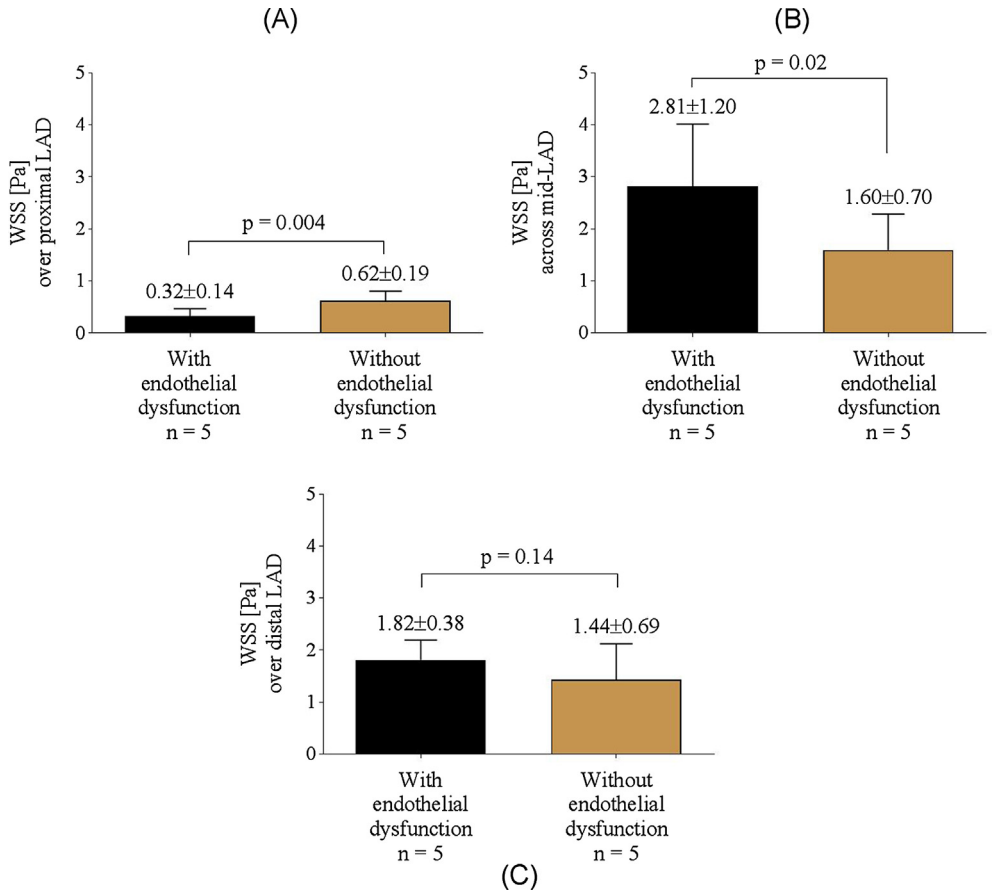

Fig. 5. WSS in patients with MB, (A) over proximal LAD, (B) across mid-LAD and (C) over distal LAD.

difference was found in the proximal WSS of those with MB compared to those without MB (Figs. 5A and 6A). Although there is not a critical value below which shear stress is considered low, based on previous experimental and human data, shear stress can be categorised as low if it is less than 1 Pa (Malek et al., 1999; Gimbrone et al., 2000; Chatzizisis et al., 2011; Samady et al., 2011; Eshtehardi et al., 2012; Corban et al., 2014). This is also supported by Kumar et al. (2018) who showed that shear stress value of <1 Pa had the highest estimated probability of severe endothelial dysfunction in patients without obstructive CAD.

We also showed that WSS in the segments proximal to MB was significantly lower than that in the bridge segments (Fig. 5). To explain this, a new CFD modelling was undertaken for the representative artery of Fig. 1 without the presence of MB such that the vessel compression caused by bridging was artificially removed. As illustrated in Fig. 8, flow recirculation zones exist in proximal segment of the model with MB (Fig. 8A) whereas they are absent in the model without MB (Fig. 8B). This may indicate why WSS is low in segments proximal to the bridge.

4.2. Endothelial dysfunction and high WSS

As with the low shear, there are no cut-off points to define high shear stresses; however, according to previous studies in patients with non-obstructive CAD (Sakamoto et al., 2006; Wentzel et al., 2012, Kumar et al., 2018; Siasos et al., 2018), WSS of 1–2.5 Pa can be considered physiological and WSS greater than 2.5 Pa can be considered high. We showed in MB patients that the level of mid-vessel shear stress changes from physiological to high when the endothelial cells become dysfunctional (Fig. 5B). However mid-vessel shear stress in patients without MB remains in physiological level despite the presence of endothelial dysfunction (Fig. 6B). High shear stress exerts protective properties on endothelial cells by activating vasodilatory, antioxidant, antithrombotic, anti-adherent and antiangiogenic responses (Sakamoto et al., 2006; Wentzel et al., 2012). Therefore, it would be expected that in MB patients endothelial dysfunction would only be seen in the proximal segment of MB where shear is low and oscillatory, and not beneath the myocardial bridge where shear is high. However, this is not the case based on several in-vivo studies (Kim et al., 2008; Kuhn et al., 1991; Zoghi et al., 2006) as well as our findings where markedly greater paradoxical vasoconstriction was observed in the bridge segment. One proposed mechanism is that an excessive increase in shear stress may alter the release of two most potent vasoactive substances from endothelial cells; NO vasodilator and endothelin-1 (ET-1) vasoconstrictor (Preter et al., 2001). In other words, high shear stress not only stimulates antioxidant systems and NO release from endothelial cells but also increases ET-1 and endogenous oxidative stress. Hence, in greatly exaggerated shear stress, a detrimental increase in oxidative stress may overcome the protective effects, which may be the case in MB with high shear conditions.

4.3. Clinical implications

Twenty to fifty percent of patients with persistent chest pain undergoing coronary angiography have non-obstructive CAD. Almost two-thirds of these patients have evidence of endothelial dysfunction (Radico et al., 2014; Sara et al., 2015), and up to 19% of them have a MB (Hostiuc et al., 2018). This indicates the impor-

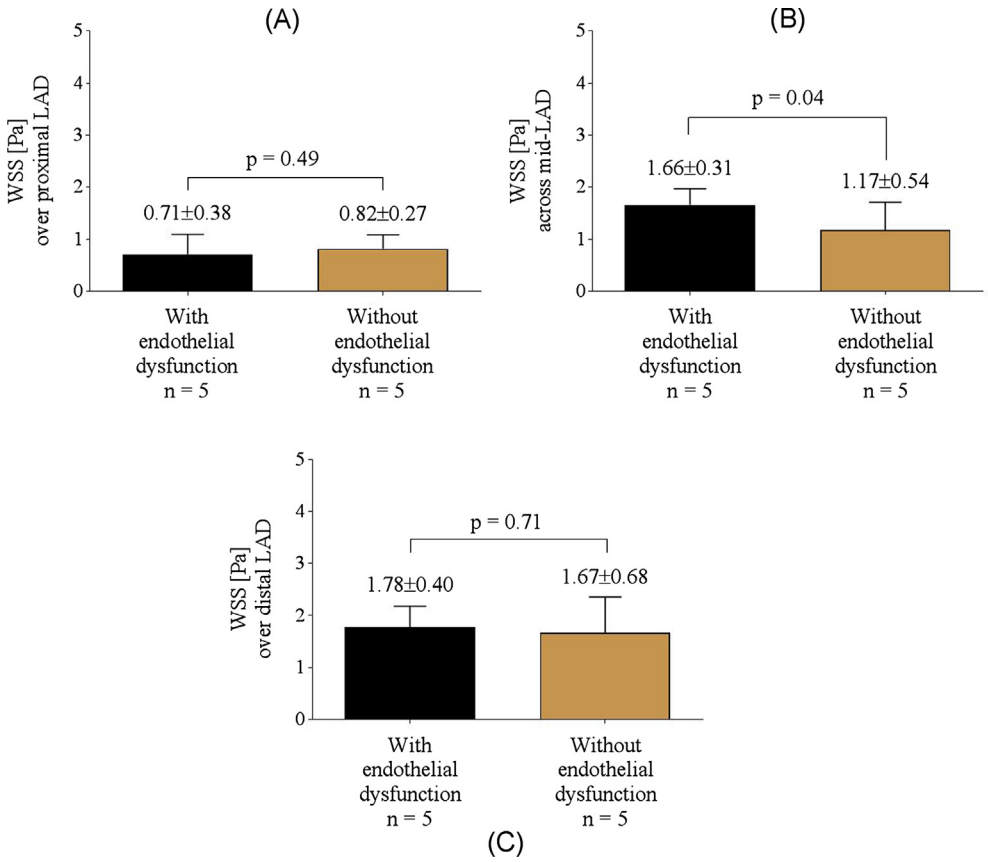

Fig. 6. WSS in patients without MB, (A) over proximal LAD, (B) across mid-LAD and (C) over distal LAD.

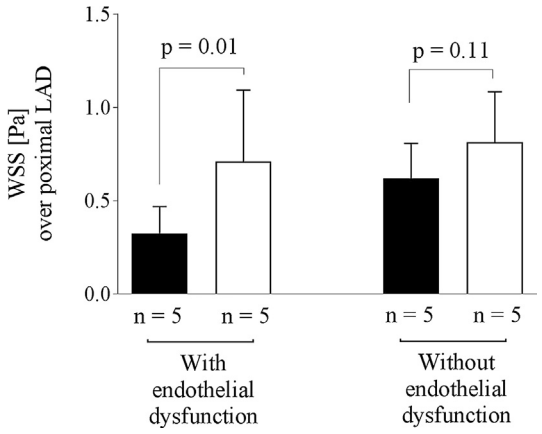

Fig. 7. Comparison between WSS over proximal LAD. "n" indicates number of patients in each group.

tance of investigating the shear and endothelial dysfunction relationship in these patients. The clinical importance of our findings can be seen from two aspects:

(i) When analysing coronary vessels regardless of presence or absence of MB

Prognostic studies have shown that low WSS promotes coronary plaque development and that patients with endothelial dysfunction have adverse cardiovascular events (Stone et al., 2003, 2007; Samady et al., 2011). We showed that shear stress in the proximal segments with endothelial dysfunction was significantly lower than that in the matched segments with normal endothelium. These findings that are in agreement with previous studies (Kumar et al., 2018; Siasos et al., 2018) warrant future clinical studies to assess whether patients with non-obstructive CAD with both endothelial dysfunction and low shear stress should undergo more intense risk-reduction therapies.

(ii) When analysing coronary vessels based on the presence or absence of MB

We showed that coronary vessels without MB had lower WSS in proximal segments with endothelial dysfunction as compared to the matched segments with normal endothelium; however, the difference was statistically insignificant. In other words, the presence of endothelial dysfunction in vessels without MB was associated with a non-significant reduction in proximal shear. In contrast, in the presence of MB the amount of reduction in WSS in proximal segments with endothelial dysfunction was substantially greater. Previous studies (Kumar et al., 2018; Siasos et al., 2018) that explored the shear and endothelial dysfunction relationship in patients with non-obstructive CAD did not exclude vessels with MB from their cohort. Our findings demonstrate that the presence of MB significantly contributes to low WSS and endothelial dysfunction relationship and support the hypothesis that MB along with endothelial dysfunction may be an indicator of pathologically low shear stress. However, this warrants further investigation.

4.4. Study limitations

This study has several limitations. Firstly, this is a single centre study and there is a relatively small number of patients. Secondly, flow was assumed to be Newtonian. It is accepted that blood is a

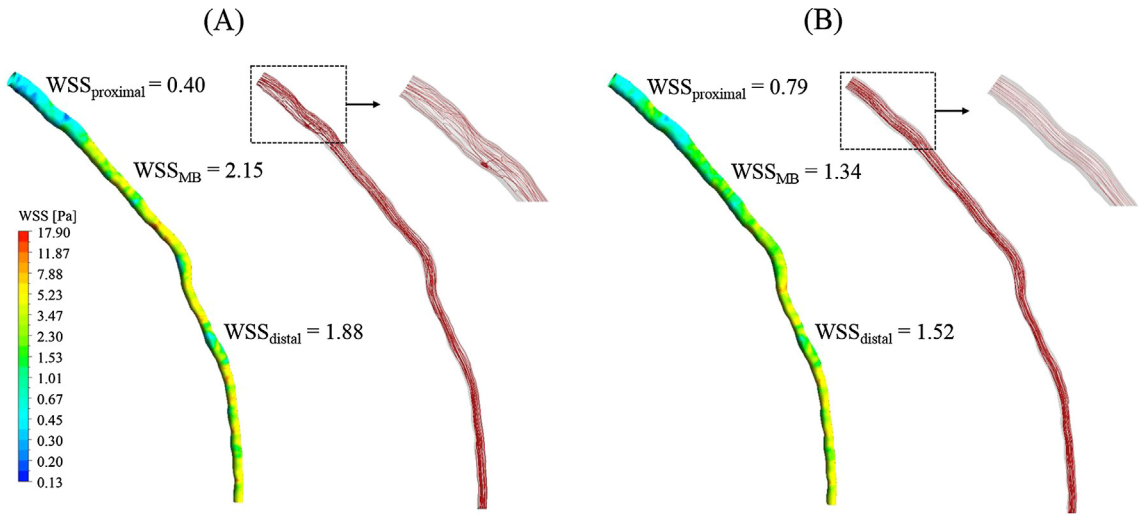

Fig. 8. WSS contours and flow streamline patterns for the representative patient of Fig. 1, (A) with MB, (B) without MB.

non-Newtonian suspension of cells in plasma and behaves like a non-Newtonian fluid in low shear rates. However, treating the blood as a Newtonian fluid is an acceptable assumption in vessels with diameter greater than approximately 0.5 mm (McDonald, 1960). Thirdly, the effect of cardiac motion was not accounted for. Theodorakakos et al. (2008) demonstarted that cardiac motion has negligible effects on coronary artery haemodynamics; however, other studies showed that the cardiac motion may significantly affect WSS (Ramaswamy et al., 2004, 2006). Fourthly, the effect of side branches was not accounted for. However, the aim of this study was to isolate the effects of MB on haemodynamic parameters, and it is therefore acceptable to ignore side branches.

5. Conclusions

Endothelial dysfunction in the proximal segment of MB may be linked to the low shear stress whereas damage to the endothelial cells beneath the myocardial bridge may be related to excessive increase in shear stress in the bridge segment.

Funding

Associate Professor Yong was supported by a Heart Foundation of Australia Future Leader Fellowship (ID 100448) and a Sir Roy McCaughey Grant from the RACP. Professor Kritharides was supported by a National Health and Medical Research Council program grant (ID 1037903).

Conflict of interest statement

The authors have no conflicts of interest to declare.

Appendix A. Supplementary material

Supplementary data to this article can be found online at https://doi.org/10.1016/j.jbiomech.2019.01.021.

References

Asakura, T., Karino, T., 1990. Flow patterns and spatial distribution of atherosclerotic lesions in human coronary arteries. Circ. Res. 66, 1045–1066.
Bourassa, M.G., Butnaru, A., Lespérance, J., Tardif, J.C., 2003. Symptomatic myocardial bridges: overview of ischemic mechanisms and current diagnostic and treatment strategies. J. Am. Coll. Cardiol. 41 (3), 351–359.
Chatzizisis, Y.S., Baker, A.B., Sukhova, G.K., Koskinas, K.C., Papafaklis, M.I., Beigel, R., Jonas, M., Coskun, A.U., Stone, B.V., Maynard, C., Shi, G.P., Libby, P., Feldman, C.L., Edelman, E.R., Stone, P.H., 2011. Augmented expression and activity of extracellular matrix-degrading enzymes in regions of low endothelial shear stress colocalize with coronary atheromata with thin fibrous caps in pigs. Circulation 123, 621–630.
Chatzizisis, Y.S., Giannoglou, G.D., 2009. Myocardial bridges are free from atherosclerosis: overview of the underlying mechanisms. Can. J. Cardiol. 25, 219–222.
Corban, M.T., Hung, O.Y., Eshtehardi, P., Rasoul-Arzrumly, E., McDaniel, M., Mekonnen, G., Timmins, L.H., Lutz, J., Guyton, R.A., Samady, H., 2014. Myocardial bridging. J. Am. Coll. Cardiol. 63, 2346–2355.
Ding, H., Yang, Q., Shang, K., Lan, H., Lv, J., Liu, Z., Liu, Y., Sheng, L., Zeng, Y., 2017. Estimation of shear stress by using a myocardial bridge-mural coronary artery simulating device. Cardiol. J. 24 (5), 530–538.
Doriot, P.A., Dorsaz, P.A., Noble, J., 2007. Could increased axial wall stress be responsible for the development of atheroma in the proximal segment of myocardial bridges? Theor. Biol. Med. Model. 4, 29.
Eshtehardi, P., McDaniel, M.C., Suo, J., Dhawan, S.S., Timmins, L.H., Binongo, J.N., Golub, L.J., Corban, M.T., Finn, A.V., Oshinski, J.N., Quyyumi, A.A., Giddens, D.P., Samady, H., 2012. Association of coronary wall shear stress with atherosclerotic plaque burden, composition, and distribution in patients with coronary artery disease. J. Am. Heart Assoc. 1, e002543.
Ferrari, M., Werner, G.S., Bahrmann, P., Richartz, B.M., Figulla, H.R., 2006. Turbulent flow as a cause for underestimating coronary flow reserve measured by Doppler guide wire. Cardiovasc. Ultrasound 4, 14.
Ge, J., Jeremias, A., Rupp, A., Abels, M., Baumgart, D., Liu, F., Haude, M., Görge, G., Von Birgelen, C., Sack, S., 1999. New signs characteristic of myocardial bridging demonstrated by intracoronary ultrasound and Doppler. Eur. Heart J. 20, 1707–1716.
Gibson, C.M., Diaz, L., Kandarpa, K., Sacks, F.M., Pasternak, R.C., Sandor, T., Feldman, C., Stone, P.H., 1993. Relation of vessel wall shear stress to atherosclerosis progression in human coronary arteries. Arterioscler. Thromb. Vasc. Biol. 13, 310–315.
Gimbrone Jr., M.A., Topper, J.N., Nagel, T., Anderson, K.R., Garcia-Cardena, G., 2000. Endothelial dysfunction, hemodynamic forces, and atherogenesis. Ann. NY Acad. Sci. 902. 230–9; discussion 239–40.
Glagov, S., Zarins, C., Giddens, D.P., Ku, D.N., 1988. Hemodynamics and atherosclerosis: insights and perspectives gained from studies of human arteries. Arch. Pathol. Lab. Med. 112, 1018–1031.
Hostiuc, S., Negoi, I., Rusu, M.C., Hostiuc, M., 2018. Myocardial bridging: a meta-analysis of prevalence. J. Forensic Sci. 63 (4), 1176–1185.
Ishii, T., Hosoda, Y., Osaka, T., Imai, T., Shimada, H., Takami, A., Yamada, H., 1986. The significance of myocardial bridge upon atherosclerosis in the left anterior descending coronary artery. J. Pathol. 148, 279–291.
Javadzadegan, A., Moshfegh, A., Fulker, D., Barber, T., Qian, Y., Kritharides, L., Yong, A.S.C., 2018. Development of a computational fluid dynamics model for myocardial bridging. J. Biomech. Eng. 140 (9), 091010.
Kim, J.W., Seo, H.S., Na, J.O., Suh, S.Y., Choi, C.U., Kim, E.J., Rha, S.W., Park, C.G., Oh, D. J., 2008. Myocardial bridging is related to endothelial dysfunction but not to plaque as assessed by intracoronary ultrasound. Heart 94, 765–769.
Kuhn, F.E., Reagan, K., Mohler, E.R., Satler, L.F., Lu, D.Y., Rackley, C.E., 1991. Evidence for endothelial dysfunction and enhanced vasoconstriction in myocardial bridges. Am. Heart J. 122, 1764–1766.
Kumar, A., Hung, O.Y., Piccinelli, M., Eshtehardi, P., Corban, M.T., Sternheim, D., Yang, B., Lefieux, A., Molony, D.S., Thompson, E.W., Zeng, W., Bouchi, Y., Gupta, S., Hosseini, H., Raad, M., Ko, Y.A., Liu, C., McDaniel, M.C., Gogas, B.D., Douglas, J.

S., Quyyumi, A.A., Giddens, D.P., Veneziani, A., Samady, H., . Low coronary wall shear stress is associated with severe endothelial dysfunction in patients with nonobstructive coronary artery disease. JACC Cardiovasc. Interv. 11 (20), 2072–2080.
Lee, B.K., Lim, H.S., Fearon, W.F., Yong, A.S., Yamada, R., Tanaka, S., Lee, D.P., Yeung, A.C., Tremmel, J.A., 2015. Invasive evaluation of patients with angina in the absence of obstructive coronary artery disease. Circulation 131 (12), 1054–1060.
Malek, A.M., Alper, S.L., Izumo, S., 1999. Hemodynamic shear stress and its role in atherosclerosis. JAMA 282, 2035–2042.
Masuda, T., Ishikawa, Y., Akasaka, Y., Itoh, K., Kiguchi, H., Ishii, T., 2001. The effect of myocardial bridging of the coronary artery on vasoactive agents and atherosclerosis localization. J. Pathol. 193, 408–414.
McDonald, D., 1960. Blood flow in arteries. Quart. J. Exp. Physiol. Cognate Med. Sci. 60. 65 65.
Menter, F.R., 1994. Two-equation eddy-viscosity turbulence models for engineering applications. AIAA J. 32, 1598–1605.
Menter, F.R., Langtry, R., Völker, S., 2006. Transition modelling for general purpose CFD codes. Flow Turbul. Combust. 77, 277–303.
Nikolić, D., Radović, M., Aleksandrić, S., Tomašević, M., Filipović, N., 2014. Prediction of coronary plaque location on arteries having myocardial bridge, using finite element models. Comput. Methods Programs Biomed. 117 (2), 137–144.
Prakash, S., Ethier, C.R., 2001. Requirements for mesh resolution in 3D computational hemodynamics. J. Biomech. Eng. 123, 134–144.
Preterre, D., Morin, J., Richard, V., Thuillez, C., 2001. Year Sheer stress and partial oxygen pressure independently affect NO release and redox state in cultured rat coronary endothelial cells. Eur. Heart J.
Puri, R., Leong, D.P., Nicholls, S.J., Liew, G.Y.L., Nelson, A.J., Carbone, A., Copus, B., Wong, D.T., Beltrame, J.F., Worthley, S.G., Worthley, M.I., 2015. Coronary artery wall shear stress is associated with endothelial dysfunction and expansive arterial remodelling in patients with coronary artery disease. EuroIntervention 10, 1440–1448.
Radico, F., Cicchitti, V., Zimarino, M., De Caterina, R., 2014. Angina pectoris and myocardial ischemia in the absence of obstructive coronary artery disease: practical considerations for diagnostic tests. J. Am. Coll. Cardiol. Intv. 7, 453–463.
Ramaswamy, S.D., Vigmostad, S.C., Wahle, A., Lai, Y.G., Olszewski, M.E., Braddy, K.C., Brennan, T.M., Rossen, J.D., Sonka, M., Chandran, K.B., 2006. Comparison of left anterior descending coronary artery hemodynamics before and after angioplasty. J. Biomech. Eng. 128 (1), 40–48.
Ramaswamy, S.D., Vigmostad, S.C., Wahle, A., Lai, Y.G., Olszewski, M.E., Braddy, K.C., Brennan, T.M., Rossen, J.D., Sonka, M., Chandran, K.B., 2004. Fluid dynamic analysis in a human left anterior descending coronary artery with arterial motion. Ann. Biomed. Eng. 32 (12), 1628–1641.
Sakamoto, N., Ohashi, T., Sato, M., 2006. Effect of fluid shear stress on migration of vascular smooth muscle cells in cocultured model. Ann. Biomed. Eng. 34, 408–415.
Samady, H., Eshtehardi, P., McDaniel, M.C., Suo, J., Dhawan, S.S., Maynard, C., Timmins, L.H., Quyyumi, A.A., Giddens, D.P., 2011. Coronary artery wall shear stress is associated with progression and transformation of atherosclerotic plaque and arterial remodeling in patients with coronary artery disease. Circulation 124, 779–788.
Sara, J.D., Widmer, R.J., Matsuzawa, Y., Lennon, R.J., Lerman, L.O., Lerman, A., 2015. Prevalence of coronary microvascular dysfunction among patients with chest pain and nonobstructive coronary artery disease. J. Am. Coll. Cardiol. 8, 1445–1453.
Sawchuk, A.P., Unthank, J.L., Davis, T.E., Dalsing, M.C., 1994. A prospective, in vivo study of the relationship between blood flow hemodynamics and atherosclerosis in a hyperlipidemic swine model. J. Vasc. Surg. 19, 58–64.
Siasos, G., Sara, J.D., Zaromytidou, M., Park, K.H., Coskun, A.U., Lerman, L.O., Oikonomou, E., Maynard, C.C., Fotiadis, D., Stefanou, K., Papafaklis, M., Michalis, L., Feldman, C., Lerman, A., Stone, P.H., 2018. Local low shear stress and endothelial dysfunction in patients with nonobstructive coronary atherosclerosis. J. Am. Coll. Cardiol. 71 (19), 2092–2102.
Stone, P.H., Coskun, A.U., Kinlay, S., Clark, M.E., Sonka, M., Wahle, A., Ilegbusi, O.J., Yeghiazarians, Y., Popma, J.J., Orav, J., Kuntz, R.E., Feldman, C.L., 2003. Effect of endothelial shear stress on the progression of coronary artery disease, vascular remodeling, and in-stent restenosis in humans: in vivo 6-month follow-up study. Circulation 108, 438–444.
Stone, P.H., Coskun, A.U., Kinlay, S., Popma, J.J., Sonka, M., Wahle, A., Yeghiazarians, Y., Maynard, C., Kuntz, R.E., Feldman, C.L., 2007. Regions of low endothelial shear stress are the sites where coronary plaque progresses and vascular remodelling occurs in humans: an in vivo serial study. Eur. Heart J. 28, 705–710.
Suwaidi, J.A., Hamasaki, S., Higano, S.T., Nishimura, R.A., Holmes, D.R., Lerman, A., 2000. Long-term follow-up of patients with mild coronary artery disease and endothelial dysfunction. Circulation 101, 948–954.
Theodorakakos, A., Gavaises, M., Andriotis, A., Zifan, A., Liatsis, P., Pantos, I., Efstathopoulos, E.P., Katritsis, D., 2008. Simulation of cardiac motion on non-Newtonian, pulsating flow development in the human left anterior descending coronary artery. Phys. Med. Biol. 53, 4875–4892.
Varghese, S.S., Frankel, S.H., Fischer, P.F., 2008. Modeling transition to turbulence in eccentric stenotic flows. J. Biomech. Eng. 130 (1), 014503.
Wang, J.C., Normand, S.L.T., Mauri, L., Kuntz, R.E., 2004. Coronary artery spatial distribution of acute myocardial infarction occlusions. Circulation 110, 278–284.
Weber, C., Noels, H., 2011. Atherosclerosis: current pathogenesis and therapeutic options. Nat. Med. 17, 1410–1422.
Wentzel, J.J., Chatzizisis, Y.S., Gijsen, F.J.H., Giannoglou, G.D., Feldman, C.L., Stone, P. H., 2012. Endothelial shear stress in the evolution of coronary atherosclerotic plaque and vascular remodelling: current understanding and remaining questions. Cardiovasc. Res. 96, 234–243.
Zoghi, M., Duygu, H., Nalbantgil, S., Kirilmaz, B., Turk, U., Ozerkan, F., Akilli, A., Akin, M., Turkoglu, C., 2006. Impaired endothelial function in patients with myocardial bridge. Echocardiography 23, 577–581.